

1 *Research Article*

2 **Testing hypotheses of diversification in Panamanian frogs and**  
3 **freshwater fishes using hierarchical approximate Bayesian**  
4 **computation with model averaging**

5 Justin C. Bagley<sup>1,2,\*</sup>, Michael J. Hickerson<sup>3,4,5</sup>, and Jerald B. Johnson<sup>6,7</sup>

6 *Author Addresses:* <sup>1</sup>Department of Biology, Virginia Commonwealth University, Richmond, VA

7 USA; <sup>2</sup>Departamento de Zoologia, Instituto de Ciências Biológicas, Universidade de Brasília,

8 Brasília, DF, Brazil; <sup>3</sup>Biology Department, City College of New York, New York, NY, USA;

9 <sup>4</sup>The Graduate Center, City University of New York, New York, NY, USA; <sup>5</sup>Division of

10 Invertebrate Zoology, The American Museum of Natural History, New York, NY, USA;

11 <sup>6</sup>Department of Biology, Brigham Young University, Provo, UT, USA; and <sup>7</sup>Monte L. Bean Life

12 Science Museum, Brigham Young University, Provo, UT, USA

13 *Author E-mail Addresses:* JCB: [jcbagley@vcu.edu](mailto:jcbagley@vcu.edu); MH: [mhickerson@ccny.cuny.edu](mailto:mhickerson@ccny.cuny.edu); JBJ:

14 [jerry.johnson@byu.edu](mailto:jerry.johnson@byu.edu).

15 *\*Corresponding author:* Dr. Justin C. Bagley; Phone: +001 (804)-828-0820; Fax: +001 (804)-

16 828-0503; E-mail: [jcbagley@vcu.edu](mailto:jcbagley@vcu.edu).

17 *Running head:* Frog & fish diversification in Panama (37 characters w/spaces)

18 *Abstract:* 234 words; *Abstract, main body, plus table and figure captions:* 7,032 words

**19 Abstract**

20 Most Neotropical frog and freshwater fish species sampled to date show phylogeographic breaks  
21 along the Pacific coast of the Isthmus of Panama, with lineages in Costa Rica and western  
22 Panama isolated from central Panama. We examine temporal patterns of diversification of taxa  
23 across this ‘western Panama isthmus’ (WPI) break to test hypotheses about the origin of species  
24 geographical distributions and genetic structuring in this region. We tested for synchronous  
25 diversification of four codistributed frog taxon-pairs and three fish taxon-pairs sharing the WPI  
26 break using hierarchical approximate Bayesian computation with model averaging based on  
27 mitochondrial DNA sequences. We also estimated lineage divergence times using full-Bayesian  
28 models. Several of our results supported synchronous divergences within the frog and freshwater  
29 fish assemblages; however, Bayes factor support was equivocal for or against synchronous or  
30 asynchronous diversification. Nevertheless, we infer that frog populations were likely isolated by  
31 one or multiple Pliocene–Pleistocene events more recently than predicted by previous models,  
32 while fish genetic diversity was structured by Pleistocene events. By integrating our results with  
33 external information from geology and elevational sea level modeling, we discuss the  
34 implications of our findings for understanding the biogeographical scenario of the diversification  
35 of Panamanian frogs and fishes. Consistent with the ‘Bermingham/Martin model’ (*Mol. Ecol.*  
36 1998, 7: 499-517), we conclude that the regional fish assemblage was fractured by processes  
37 shaping isthmian landscapes during the Pleistocene glaciations, including drainage basin  
38 isolation during lowered sea levels.

### 39 **Introduction**

40 By revealing the geographical histories of genetic lineages within species, phylogeography helps  
41 identify processes that influence the divergence, spread, and spatial-demographic fluctuations of  
42 lineages (Avise *et al.*, 1987; Avise, 2000; Kidd & Ritchie, 2006). Single-species phylogeography  
43 surveys often reveal cryptic refugia and speciation events (e.g. Avise, 2000; Soltis *et al.*, 2006;  
44 Bagley & Johnson, 2014a). By contrast, ‘comparative phylogeography’ presents a stronger  
45 approach for testing the generality of evolutionary patterns recovered within single species, often  
46 uncovering historical processes shaping species richness and genetic diversity (Arbogast &  
47 Kenagy, 2001; Hickerson *et al.*, 2010). Comparative phylogeography infers the histories of  
48 regional assemblages by testing for spatial and temporal phylogeographic congruence across  
49 codistributed species (Bermingham & Avise, 1986; Avise *et al.*, 1987; Bermingham & Martin,  
50 1998). Congruent spatiotemporal divergences across taxa can indicate a shared history of  
51 responses to historical events (Bermingham & Martin, 1998; Sullivan *et al.*, 2000).

52       Most comparative surveys in phylogeography are based on mitochondrial DNA (mtDNA)  
53 and are consequently subject to the caveats of using a single locus. Phylogeographic histories  
54 within individual species may be confounded by effects of stochastic variance in coalescent and  
55 mutational processes, natural selection, sex-biased dispersal, or reproductive success on genetic  
56 data (Avise, 1989; Edwards & Beerli, 2000; Hey & Machado, 2003; Kuo & Avise, 2005; Irwin,  
57 2012). Comparative studies guard against effects of such stochastic processes on inferences by  
58 searching for phylogeographic patterns replicated across multiple lineages (Avise, 2000; Zink,  
59 2002). This is analogous to improving evolutionary inferences through using multiple loci to  
60 estimate population parameters, multilocus models, or population/species trees across multiple  
61 gene genealogies (Edwards & Beerli, 2000; Kubatko *et al.*, 2009; Heled & Drummond, 2010).  
62 Still, comparative approaches face major challenges to distinguish among potential scenarios that

63 may have led to the observed patterns. Parameter estimates from mtDNA can suffer from low  
64 resolution, yielding wide confidence intervals that limit hypotheses testing (Edwards & Beerli,  
65 2000). The critical task of understanding the temporal framework of diversification to infer the  
66 historical biogeographical scenario underpinning spatial-genetic patterns can also be  
67 problematic, even if spatially congruent breaks are identified. Because variance in past effective  
68 population sizes ( $N_e$ ), mutation rate, and generation time create high variation in gene tree  
69 topologies and their depths (correlated with timing of their divergences; e.g. Avise, 1989;  
70 Hudson, 1990), what appear as multiple divergence events may actually reflect the obscured  
71 signal of a single event (Riddle & Hafner, 2006). Thus, comparing independent gene-tree depths  
72 and divergence time estimates can lead to erroneous inferences of multiple vicariance events.

73         To guard against potential misinterpretations of biogeographical history, it is imperative  
74 to rigorously evaluate the timing of population divergences across species. Approximate  
75 Bayesian computation (ABC) methods for phylogeography allow accounting for potentially  
76 confounding stochastic coalescent effects while estimating parameters of phylogeographic  
77 datasets in such a way that sidesteps the need to calculate explicit likelihood functions. These  
78 “likelihood-free” methods permit simultaneously estimating demographic parameters and  
79 divergence times across populations by replacing the data with summary statistics, resulting in  
80 more efficient extraction of information (e.g. Beaumont *et al.*, 2002; Hickerson *et al.*, 2007). One  
81 broadly validated ABC method for comparative phylogeography, the MTML-msBayes pipeline  
82 (Hickerson *et al.*, 2006, 2007, 2014; Huang *et al.*, 2011), permits comparing hypotheses in a  
83 parameter-rich hierarchical ABC (hABC) model using data from multiple codistributed  
84 population-pairs. This method has become widely used for testing explicit hypotheses about the  
85 timing of genetic divergences that have arisen during the assembly and diversification of

86 regional species assemblages (Leaché *et al.*, 2007; Barber & Klicka, 2010; Bell *et al.*, 2012;  
87 Dolman & Joseph, 2012; Bagley & Johnson, 2014b; Smith *et al.*, 2014). Based on simulations,  
88 some have cautioned that overly broad priors can result in low power to detect multiple  
89 divergences using MTML-msBayes (Oaks *et al.*, 2013). However, this pitfall can be avoided by  
90 graphical sampling checks as well as comparing multiple MTML-msBayes model classes  
91 (priors) using ABC model averaging to account for uncertainty in model selection (Hickerson *et*  
92 *al.*, 2014; Bagley, 2014). Other workers have also advocated leaving the summary statistics  
93 vector unsorted, as well as employing a Dirichlet-process prior as the hyperprior for the  
94 hyperparameter on the number of co-divergence events ( $\Psi$ ) in the MTML-msBayes model and  
95 relying on this hyperparameter for inference (Oaks, 2014; Oaks *et al.*, 2014; Papadopoulou &  
96 Knowles, 2015). However, our recent study using a cross-validation approach applied to  
97 simulated and empirical data, including the Panamanian datasets analyzed in the current paper,  
98 shows conclusively that choice of prior on  $\Psi$  has limited impact on inference, while re-sorting of  
99 summary statistics yields considerably more reliable results (Overcast *et al.*, 2017).

100         The Central American Isthmus has been an active area of phylogeographic research for  
101 nearly 20 years, with most studies focusing on inferring how, when, and why lineages colonized  
102 the isthmian landscape, diversified, and assembled into local communities (Bagley & Johnson,  
103 2014a). A growing catalogue of species is being identified with common phylogeographic  
104 divergences across the Pacific-coastal lowlands of the Isthmus of Panama, with lineages in Costa  
105 Rica's Golfo Dulce region and western Panama isolated from lineages in central Panama (Figs 1  
106 and 2; reviewed by Bagley & Johnson, 2014a). This pattern has become known as the 'western  
107 Panama isthmus' (WPI) break (Bagley & Johnson, 2014a). Biogeographers interpret WPI breaks  
108 in frogs as resulting from multiple dispersals of different lineages into Central America across a

109 continuous Miocene–Pliocene wet forest corridor, from both the north and the south (Savage,  
110 1966, 1982, 2002; Vanzolini & Heyer, 1985), followed by vicariance caused by the development  
111 of tropical dry forest 12–4 million years ago (Ma; ‘dry forest hypothesis’; Crawford *et al.*, 2007;  
112 Wang *et al.*, 2008). While frog fossils from the region are lacking, this scenario is supported by  
113 plant microfossils showing that modern dry forest species began appearing in central Panama up  
114 to mid-Pliocene (Graham & Dilcher, 1995; Piperno & Pearsall, 1998). Among freshwater fishes,  
115 the WPI break appears to reflect the effectiveness of rugged terrains at Soná and Azuero  
116 peninsulas (Fig. 1) as biogeographical barriers to fish lineages, which arrived in multiple  
117 northwestward waves from South America since the Neogene. Bermingham & Martin (1998)  
118 hypothesized that a corridor formed by low sea level and tectonic uplift of the isthmus as the  
119 Cocos Ridge collided with the Panama microplate by ~7 Ma (Coates & Obando, 1996) permitted  
120 ‘early’ emplacement of freshwater fish species since Miocene–Pliocene. Subsequently, they  
121 argued that high eustatic sea levels of the mid-late Pliocene ~3.5–3 Ma (Cronin & Dowsett,  
122 1991) recreated a seaway over the isthmus, causing freshwater fishes to go extinct in central  
123 Panama ~3 Ma, before final isthmus emergence (Bermingham & Martin, 1998). They  
124 hypothesized that the WPI break in fishes resulted from fragmentation due to drainage basin  
125 isolation during Pleistocene glacial periods over 2–0 Ma (Bermingham & Martin, 1998). This  
126 ‘Bermingham/Martin model’ has also been invoked to explain phylogeographic patterns in  
127 pseudoscorpions, eels, catfishes, frogs, and other taxa (e.g. Zeh *et al.*, 2003; Perdices *et al.*, 2002,  
128 2005; Weigt *et al.*, 2005; Bagley & Johnson, 2014a).

129         Clearly, previous studies generated or tested biogeographical models that provide  
130 convincing evidence for the WPI break. However, none of these studies explicitly accounted for  
131 genetic variance associated with coalescent processes, or among-lineage differences in

132 demography or mutational rates, that may have influenced the variable patterns of genetic  
133 divergences of taxa associated with the WPI break (Bermingham & Martin, 1998; Crawford *et*  
134 *al.*, 2007; see Results). Thus, the temporal pattern and underlying mechanisms of diversification  
135 across the WPI break have not yet been fully explored. Additional studies are needed to evaluate  
136 whether the pattern of genetic structuring shared among frogs and freshwater fishes in the  
137 western Panama isthmus arose synchronously or asynchronously, and to determine the timing of  
138 historical events that have shaped community assembly and genetic divergence in this region.

139         The goal of this study is to examine the temporal patterns of diversification of frogs and  
140 freshwater fishes across the WPI break to test existing hypotheses about the origin of species  
141 distributions and genetic structuring in west-Pacific Panama. We use hABC simulations with  
142 ABC model averaging, and full-Bayesian divergence time estimation, to test the alternative  
143 hypotheses of a single, synchronous pulse of diversification, versus multiple pulses of  
144 diversification, in the frog and fish assemblages across this region. In doing so, we are able to  
145 directly test the hypotheses discussed above. Support for synchronous diversification correlated  
146 to Pliocene high seas ~3.5–3 Ma would agree with frog and fish WPI divergences arising from a  
147 common history of Neogene dispersal into western Panama followed by isolation wrought by  
148 fluctuating Plio–Pleistocene sea levels, and possibly other factors (e.g. dry forests isolating the  
149 frog populations). This would support the Bermingham/Martin model as a general model of  
150 diversification applicable to frogs and freshwater fishes. By contrast, an inference of one or  
151 multiple pulses of frog diversification <4 Ma would reject the dry forest hypothesis, whereas a  
152 pulse of fish vicariance events >2 Ma would reject the Bermingham/Martin model as an  
153 explanation for fish assemblage genetic structure across the western Isthmus of Panama.

## 154 **Materials and methods**

**155 Taxon sampling and molecular data**

156 We considered all phylogeographic studies of lower Central American (Costa Rica–Panama)  
157 taxa, including studies summarized in a recent comprehensive review (Bagley & Johnson,  
158 2014a), and subsequent publications. Taxa were included in this study if they met minimum  
159 criteria for our analyses: frogs or freshwater fish species/lineages codistributed across the study  
160 area; genetic divergence at the WPI break, with at least two individuals sampled on either side;  
161 and mtDNA gene sequences available from GenBank. We focused on the mtDNA locus because  
162 it presents a rapidly evolving and coalescing genomic region that often reflects population  
163 history (Zink & Barrowclough, 2008). Also, protein-coding mtDNA genes have been widely  
164 studied in Central American taxa, permitting interspecific comparisons.

165 We obtained seven population-pair comparisons from eight taxa from our literature  
166 search (Table 1). Taxa that met our criteria included the following four lineages of frogs: the red-  
167 eyed treefrog, *Agalychnis callidryas* (Robertson & Zamudio, 2009); the dirt frog, *Craugastor*  
168 *crassidigitus* (Crawford *et al.*, 2007); the hourglass treefrog, *Dendropsophus ebraccatus*  
169 (Robertson *et al.*, 2009), and the túngara frog, *Engystomops (Physalaemus) pustulosus* (Weigt *et*  
170 *al.*, 2005). The following three freshwater fish lineages also met our criteria: the blue acara,  
171 *Andinoacara coeruleopunctatus* (McCafferty *et al.*, 2012); the Chagres catfish, *Pimelodella*  
172 *chagresi* (Bermingham & Martin, 1998; Martin & Bermingham, 2000); and headstander tetras,  
173 *Roeboides occidentalis–R. guatemalensis* (Bermingham & Martin, 1998). While their broader  
174 geographical distributions differ to varying degrees, all species/lineages are codistributed in the  
175 study area and exhibit the WPI break (Fig. 2), and most are thought to have expanded their  
176 ranges into Central America from southern source populations in eastern Panama or northern  
177 South America (Bussing, 1976, 1998; Savage, 1982, 2002; Bermingham & Martin, 1998). An

178 exception to this is *C. crassidigitus*, which more likely colonized the region from an ancestral  
179 population in the north, i.e. Nuclear Central America (Vanzolini & Heyer, 1985; Crawford &  
180 Smith, 2005). We excluded from our analyses two taxa inferred to exhibit the WPI break in  
181 previous studies, *Brachyhypopomus occidentalis* (Bermingham & Martin, 1998) and  
182 *Synbranchus marmoratus* (Perdices *et al.*, 2005). In the case of *B. occidentalis*, available mtDNA  
183 sequences had insufficient sample sizes for estimating population parameters and coalescent  
184 modeling, which require  $\geq 2$  individuals from daughter lineages on either side of the break. Also,  
185 two studies conflicted as to whether this taxon showed the WPI break (Bermingham & Martin,  
186 1998; Picq *et al.*, 2014). In *S. marmoratus*, the geographical location of the WPI break included a  
187 major north–south component of isolation across the Central Cordillera, thus the break was not  
188 as well confined to the Pacific coast as in other taxa we analyzed, making comparisons difficult.

189         A summary of sampling intensity and molecular characteristics of each dataset, and their  
190 published sources, is provided in Table 1. Our final database consisted of 109 sequences  
191 representing 10–28 individuals sampled from each of these seven species (2–16 individuals  
192 sampled from the west or east side of the break), permitting us to address the evolution of frog  
193 and freshwater fish species assemblages. Final mtDNA alignments for each species/lineage  
194 ranged from 564 to 1877 bp in length, and most (4/7) datasets contained cytochrome oxidase  
195 subunit 1 (*cox1*) ‘DNA barcode’ sequences. GenBank numbers and locality data for the samples  
196 used in each dataset are provided in Table S1. Sequence data were grouped *a priori* into  
197 populations east and west of the WPI break. We assumed HKY (Hasegawa *et al.*, 1985) models  
198 with gamma-distributed rate variation ( $\Gamma$ ) and an estimated proportion of invariant sites (*I*)  
199 wherever possible 1) because this model provides a more appropriate description of mtDNA  
200 sequence evolution (e.g. allowing recurrent mutations) than other nucleotide substitution models

201 available in the MTML-msBayes pipeline (e.g. Jukes-Cantor or equal-input), and 2) to make  
202 results comparable across analyses.

### 203 **Genetic diversity and neutrality**

204 We examined genetic diversity by calculating nucleotide diversity ( $\pi$ ; Nei, 1987) for each dataset  
205 using the ‘obsSumStats.pl’ Perl script available in the latest version of the MTML-msBayes  
206 pipeline (Huang *et al.*, 2011). To further evaluate patterns of genetic divergence across the WPI  
207 break, we estimated average % divergence between clades for all population-pairs using  
208 distances corrected using the HKY+ $\Gamma$ + $I$  substitution model in PAUP\* 4.0b10 (Swofford, 2002).  
209 In PAUP\*, we specified  $\Gamma$  and  $I$  parameter estimates derived from Bayesian coalescent gene-tree  
210 analyses of each population-pair (below). Although selective neutrality is often a valid  
211 assumption for vertebrate organellar mtDNA, this was a key assumption of our analyses; thus,  
212 we tested for mtDNA selective neutrality using McDonald & Kreitman’s (1991; MK) tests  
213 conducted in DnaSP 5 (Librado & Rozas, 2009). Closely related, congeneric outgroup taxa were  
214 included in the MK tests for each population-pair based on phylogenies in the original studies, or  
215 large-scale phylogenetic studies (see Appendix S1 for details).

### 216 **Estimating gene-tree depths using Bayesian dating**

217 To independently assess variation in gene-tree depths across WPI break taxa, we estimated times  
218 to the most recent common ancestors ( $t_{\text{MRCAS}}$ ) and their Bayesian credible intervals for each  
219 species/lineage using BEAST 1.8.2 (Drummond *et al.*, 2012). BEAST runs (100 million  
220 generations, sampled every 4000; ‘burn-in’ = 10%) started from UPGMA tree topologies,  
221 employed HKY+ $\Gamma$ + $I$  site models, and used coalescent constant size tree priors (Kingman, 1982).  
222 We evaluated the fit of different molecular clock models and investigated clock-likeness of the  
223 data by comparing results of strict-clock and relaxed-clock (uncorrelated lognormal model;

224 Drummond *et al.*, 2006) runs on each dataset. Due to uncertainty over frog mtDNA mutation  
225 rates, we specified a range of 0.1–1.3% lineage<sup>-1</sup> Myr<sup>-1</sup> (per million years) in the frog runs  
226 spanning rates of protein-coding mtDNA gene evolution documented in a broader mtDNA  
227 dataset from one of our focal taxa (Weigt *et al.*, 2005). This ‘frog rate’ spans Macey *et al.*’s  
228 (1998) Mongolian toad (*Bufo bufo*) rate of 0.69% lineage<sup>-1</sup> Myr<sup>-1</sup>, which is commonly used to  
229 date patterns of herpetofaunal diversification (Weigt *et al.*, 2005). Likewise, we specified a ‘fish  
230 rate’ of 0.17–1.4% lineage<sup>-1</sup> Myr<sup>-1</sup> in fish runs, a range spanning mutation rates estimated in 15  
231 previous studies of teleost freshwater fish mtDNA (refs. in Waters *et al.*, 1999; BurrIDGE *et al.*,  
232 2008). Rate ranges were supplied to the program as uniform priors. We summarized posterior  
233 distributions and ensured convergence and adequate effective sample sizes (all ESS >> 200)  
234 using Tracer v1.5 (available at: <http://beast.bio.ed.ac.uk/Tracer>). In TreeAnnotator 1.8.2, we  
235 summarized the posterior distribution of trees from each run by calculating a maximum clade  
236 credibility (MCC) tree annotated with median node ages from a sample of 5000 post-burn-in  
237 trees obtained using the ‘BEASTPostProc.sh’ script in PIRANHA v0.1.4 (Bagley, 2017).

### 238 **Tests for synchronous diversification**

239 We tested the hypotheses of a single, synchronous pulse of diversification versus multiple pulses  
240 of diversification of the seven population-pairs across the WPI break under a coalescent model,  
241 using the MTML-msBayes pipeline (Huang *et al.*, 2011). Because hyperprior ABC samplers like  
242 msBayes can inefficiently sample from the prior when overly broad prior bounds are used,  
243 biasing them towards inferring simultaneous diversification (Oaks *et al.*, 2013), we used ABC  
244 model averaging on candidate priors and visual checks for prior sampling efficiency to help  
245 overcome this issue (Hickerson *et al.*, 2014). Also, following recommendations for MTML-  
246 msBayes analyses of small numbers of taxon/population-pairs in an extensive simulation study

247 (Overcast *et al.*, 2017), we ran MTML-msBayes with the default summary statistics and sorting  
248 algorithm, and we relied principally on the  $\Omega$  hyperparameter (see below) for inference and  
249 hypotheses tests. Our MTML-msBayes analysis consisted of a four-step procedure similar to  
250 Hickerson *et al.* (2014). First, we developed four prior sets, or model classes ( $M_1$ – $M_4$ ), to  
251 compare using model averaging. Each model class consisted of one of two uniformly distributed  
252 priors on population divergence times ( $\tau$ ), ancestral population size ( $\theta_A$ ), and daughter population  
253 size parameters ( $\theta_D$ ; Table 2). Second, we obtained 5 million random (simulated) samples from  
254 each model class specified by a discrete uniform hyperprior distribution  $\Pr(M_k)=1/4$ . We visually  
255 checked for efficient prior sampling by conducting principal components analysis on 1000 prior  
256 draws from each model class in R. Third, we obtained the ABC joint posterior distribution using  
257 the default summary statistic vector ( $D$ ) from MTML-msBayes and rejection sampling to  
258 identify the 1000 closest Euclidean distances between the observed summary statistics ( $D^*$ ) for  
259 the data and  $D_i$  calculated from 20 million random draws across all four priors ( $M_1$ – $M_4$ ).  
260 However, prior to rejection sampling, we rescaled the dispersion index of population divergence  
261 times [ $\Omega = Var(\tau)/E(\tau)$ ; the ratio of variance to the mean of the divergence times] and the mean  
262 assembly-wide divergence time,  $E(\tau)$ , from models with smaller upper  $\theta_D$  prior bound values  
263 (frog and fish  $M_1$ ,  $M_2$ , and  $M_4$ ) to have the same coalescent units as the other model,  $M_3$   
264 (Hickerson *et al.*, 2014). Resulting estimates of  $\Omega$  and  $E(\tau)$  were weighted by Bayesian model  
265 averaging (Hickerson *et al.*, 2014). Last, we conducted hypothesis testing by comparing  
266 hyperposterior probability distributions of  $\Omega$  estimates, to determine whether the data supported  
267 single or multiple diversification periods.

268         We conducted hypothesis testing by comparing posterior probabilities of the  
269 hyperparameter estimates under a ‘null’ scenario of asynchronous diversification ( $\Omega > 0.01$ )

270 versus the alternative of synchronous diversification ( $\Omega \leq 0.01$ ) (Hickerson *et al.*, 2006, 2007;  
271 Bell *et al.*, 2012; Bagley & Johnson, 2014b) and subsequently calculating  $B_{10}$  Bayes factors  
272 under the parameter thresholds above while accounting for prior support for the hypotheses,  
273 using  $B_{10}$  “weight of evidence” criteria in Jeffreys (1961) and Kass & Raftery (1995). We  
274 estimated mean assemblage-wide divergence times by converting model-averaged  $E[\tau]$  estimates  
275 (in coalescent units of  $4N_{\text{ave}}$  generations) to absolute time ( $T_{\text{div}}$ ) using the equation  $T_{\text{div}} =$   
276  $E[\tau] \times (\theta_{\text{ave}} / \mu)$ , where  $\mu$  is the assumed mutation rate per site per generation and  $\theta_{\text{ave}}$  (per site) is  
277 the mean of the upper  $\theta$  prior. Conversions used mutation rates equivalent to 0.7% lineage<sup>-1</sup> Myr<sup>-1</sup>  
278 and 0.785% lineage<sup>-1</sup> Myr<sup>-1</sup>, the median rates of uniform ‘frog rate’ and ‘fish rate’ priors used  
279 in our BEAST analyses. We assumed an average generation time of 1 year, which was also used  
280 in previous studies of our focal taxa (e.g. Weigt *et al.*, 2005; Robertson & Zamudio, 2009;  
281 McCafferty *et al.*, 2012), and we acknowledge that divergence time estimates are sensitive to  
282 generation times. Shell and R scripts used during our MTML-msBayes analyses are accessioned  
283 in Mendeley Data (Bagley & Hickerson, 2018).

## 284 **Results**

### 285 **Genetic diversity and neutrality**

286 Clades examined here had considerably variable levels of genetic variation, with  $\pi$  values  
287 ranging 6-fold from 0.0093 in *A. callidryas* to 0.0645 in *C. crassidigitus* (Table 1); these same  
288 two taxa exhibited the lowest and highest levels of sequence divergence, respectively. There was  
289 also more variation in nucleotide diversity among frogs than among freshwater fishes. Likewise,  
290 genetic divergences based on HKY+ $\Gamma$ + $I$  corrected distances between clades on either side of the  
291 break ranged from 4.6% up to a maximum of 13.9% among frog taxa, whereas that among fish  
292 species/lineages showed a more limited range from 2.4% to 6.4% (Table 1). Consistent with the

293 assumptions of our analyses, MK tests did not reveal departures from selective neutrality within  
294 any of the mtDNA datasets (Fisher's exact test  $P > 0.10$ ; Appendix S1).

### 295 **Estimating gene-tree depths using Bayesian dating**

296 Estimated  $t_{\text{MRCAS}}$  for each of the seven population-pairs were consistent across multiple BEAST  
297 runs, which had ESS values  $>500$  for nearly all parameters. Results also were similar across  
298 strict-clock and relaxed-clock runs; however, we only present the results of the strict-clock  
299 analyses because 95% highest posterior densities (HPDs) of 'uclid.stdev' (standard deviation of  
300 the relaxed clock) abutted zero, indicating that the data could not reject strict clock models. The  
301 mitochondrial MCC time trees had variable gene-tree depths (Fig. S1), and geometric mean  
302  $t_{\text{MRCA}}$  estimates (closer to peak likelihood values than the means) varied substantially across  
303 species/lineages, ranging from 1.71 Ma in *A. coeruleopunctatus* to 10.79 Ma in *C. crassidigitus*  
304 (Fig. 3; frog geometric mean  $t_{\text{MRCA}}$  range: 3.78–10.80 Ma; fish geometric mean  $t_{\text{MRCA}}$  range:  
305 1.71–4.88 Ma). Consistent with patterns of DNA polymorphism above,  $t_{\text{MRCAS}}$  of the fish  
306 lineages exhibited less variation with a much narrower region of overlap in their coalescence  
307 times (1.92–5.57 Ma) as compared with that of the frog lineages (3.88–14.39 Ma), although the  
308 frog  $t_{\text{MRCAS}}$  also overlapped substantially (Fig. 3).

### 309 **Tests for synchronous diversification**

310 Projecting the observed data into principal components calculated from summary statistics  
311 randomly drawn from each model class showed that MTML-msBayes efficiently sampled our  
312 prior distributions (Fig. S2). Observed data points also had similar positions across model  
313 classes, suggesting different priors were similarly good samplers for the data. Below we report  
314 results based on  $\Omega$  posteriors derived from local linear regression (Beaumont *et al.*, 2002).

315 We found that the modes of model-averaged posterior estimates of hyperparameter  $\Omega$   
316 were consistent with synchronous divergences within the frog and fish assemblages (frog  $\Omega$   
317 mode = 0.0036; fish  $\Omega$  mode = 0.0017; Table 2; Fig. 4). In agreement with this pattern,  $\Omega = 0$  fell  
318 within the credible intervals (95% HPD) of each of the model-averaged  $\Omega$  distributions. The  
319 best-supported models also indicated synchronous divergence of the frog and the fish lineages  
320 based on posterior modal  $\Omega$  values of 0.0013 and 0.0047, respectively. Despite this, model  
321 comparisons using Bayes factors for the ABC model-averaging results indicated that the data  
322 provided equivocal support for or against either model. Bayes factors were around a value of 1  
323 for both the synchronous diversification model (frog  $B_{10} = 1.14$  for  $\Omega < 0.01$  versus  $\Omega > 0.01$ ;  
324 fish  $B_{10} = 1.33$  for  $\Omega < 0.01$  versus  $\Omega > 0.01$ ) as well as the asynchronous diversification model  
325 (frog  $B_{10} = 0.88$  for  $\Omega > 0.01$  versus  $\Omega < 0.01$ ; fish  $B_{10} = 0.75$  for  $\Omega > 0.01$  versus  $\Omega < 0.01$ ).  
326 Bayes factors were technically less than 1 for two or more divergences, but at best this provides  
327 very weak negative evidence for asynchronous divergence (Jeffreys, 1961; Kass & Raftery,  
328 1995). Likewise, posterior probabilities for the best-supported models were low ( $<0.5$ ) and  
329 corresponding Bayes factors for synchronous diversification were weak, being approximately  
330 less than or equal to 1.

331 Based on model-averaging, the modes of assemblage  $E(\tau)$  for the frog lineages and fish  
332 lineages were 0.106 (95% HPD = 0.056–0.139) and 0.054 (95% HPD = 0.022–0.079),  
333 respectively (Fig. 4). When converted to absolute time using the median frog and fish mutation  
334 rates above, these peak-likelihood estimates correspond to modal dates of 3.09 Ma (95% HPD =  
335 1.62–4.03 Ma) in the Pliocene to early Pleistocene for the frog divergences and 1.36 Ma (95%  
336 HPD = 0.56–2.021 Ma) in the early-mid Pleistocene for the fish divergences (Fig. 4).

## 337 Discussion

338 Determining whether species assemblages experienced shared evolutionary responses to  
339 historical geological and climate-change events is a central but challenging goal of comparative  
340 phylogeography (Avice, 2000; Sullivan *et al.*, 2000; Arbogast & Kenagy, 2001). Multi-taxon  
341 hABC methods for comparative phylogeography (e.g. Hickerson *et al.*, 2006, 2007, 2014; Huang  
342 *et al.*, 2011) permit testing explicit hypotheses about the timing of genetic divergences that have  
343 arisen during the assembly and diversification of regional species assemblages (Leaché *et al.*,  
344 2007; Barber & Klicka, 2010; Bell *et al.*, 2012; Dolman & Joseph, 2012; Bagley & Johnson,  
345 2014b; Bagley, 2014; Smith *et al.*, 2014). We used hABC coalescent models and full-Bayesian  
346 divergence dating to investigate temporal patterns of diversification of frogs and freshwater  
347 fishes across the WPI phylogeographic break (Figs 1 and 2; Bagley & Johnson, 2014a) to test  
348 two *a priori* hypotheses about the origin of species distributions and genetic structuring along the  
349 Pacific coast of Panama.

350         Several aspects of our results indicated that the frog and freshwater fish assemblages each  
351 experienced a synchronous pulse of diversification in this region during the late Neogene to  
352 Quaternary. This was supported by overlap in estimated  $t_{\text{MRCAS}}$  for the taxon-pairs (Fig. 3),  
353 strong peaks in the  $\Omega$  posteriors near zero (Fig. 4) and credible intervals including zero (Table 2),  
354 and peak-likelihoods and credible intervals of assemblage  $E(\tau)$ . By contrast, Bayes factor model  
355 selection indicated that the data provide only a marginal accumulation of evidence in favor of  
356 synchronous diversification and against the null scenario of asynchronous diversification. The  
357 msBayes approach has been shown to correctly reject synchronous diversification using only  
358 mtDNA and summary statistics such as those used herein (e.g. Hickerson *et al.*, 2006; Huang *et*  
359 *al.*, 2011; Hickerson *et al.*, 2014), and visual checks suggested that our priors were efficient  
360 samplers of the data (Fig. S2). Moreover, we avoided the problem of overly broad or narrow  $\tau$

361 priors (e.g. in Leaché *et al.*, 2007; Oaks *et al.*, 2013), which can cause ABC samplers to explore  
362 parameter space exceeding saturation effects on mitochondrial genes (Hickerson *et al.*, 2014), by  
363 matching the upper bounds of these priors to empirical estimates from the data. As a result, we  
364 conclude that additional genetic data from unlinked loci or additional species, or improved  
365 methods for hABC or Bayes factor estimation, are needed to more confidently assess the timing  
366 and number of events at the WPI break in these taxa. Nevertheless, the much narrower credible  
367 intervals of our assemblage divergence times relative to the Bayesian gene-tree depths inferred in  
368 BEAST (Fig. 3) indicate that accounting for coalescent processes and changes in population  
369 sizes through time in our models yielded much more precise estimated divergence times across  
370 the WPI break than were previously available. Assuming that peaks in  $\Omega$  and  $E(\tau)$  contain one or  
371 multiple clusters of population divergence events, and acknowledging limitations and caveats of  
372 our mtDNA data (see Introduction and Appendix S1 section 3), we use our Bayesian assemblage  
373  $E(\tau)$  estimates to draw broad conclusions about the timing of diversification in these two  
374 assemblages and conduct hypotheses tests. We also discuss implications of our results for  
375 understanding the historical biogeography and diversification of Panamanian frog and freshwater  
376 fish species assemblages.

377         The dry forest hypothesis predicts that the timing of diversification of frogs across the  
378 WPI break was marked by the transition from wet tropical forest in the middle Cenozoic to drier  
379 forest habitats along the Pacific coast of Panama by >4 Ma according to paleobotanical data  
380 (Graham & Dilcher, 1995; Piperno & Pearsall, 1998), and up to 12 Ma based on mtDNA  
381 phylogenetic dating analyses (Crawford *et al.*, 2007; Wang *et al.*, 2008). Against these  
382 predictions, we inferred that frog diversification across the WPI break occurred more recently,  
383 around 3.09 Ma (Figs 3 and 4). Credible intervals for model-averaged assemblage  $E(\tau)$  from

384 MTML-msBayes slightly overlapped the predicted interval, by only ~31 thousand years (kyr);  
385 thus, we do not reject the dry forest hypothesis outright. However, modal  $\Omega$  and assemblage  $E(\tau)$   
386 estimates favor the conclusion that the fracturing of western and eastern Pacific Panama frog  
387 assemblage coincided with one or multiple historical events occurring after 4 Ma, during the late  
388 Pliocene–early Pleistocene. Differences between frog divergence times inferred by earlier  
389 workers and this study likely owe in part to differences in sampling and methods used. Crawford  
390 *et al.* (2007) dated the isolation of Golfo Dulce *Craugastor* populations using analyses that  
391 combined interspecific samples and employed strict molecular-clock and nonparametric rate  
392 smoothing methods. Thus, unlike population divergence times we estimated in MTML-msBayes,  
393 earlier estimates of Golfo Dulce frog divergence times were based on gene divergences, which  
394 are more apt to overestimate the timing of diversification (e.g. Edwards & Beerli, 2000).

395         While we cannot reject the dry forest hypothesis outright, our results are more consistent  
396 with the interpretation that Plio–Pleistocene sea level highstands limited frog dispersion and gene  
397 flow across the region, as predicted by the Bermingham/Martin model (Bermingham & Martin,  
398 1998). The Pliocene warm period was a time of reduced global ice volume, stable and warmer  
399 temperatures, and widely fluctuating sea levels 3.5–2.5 Ma (Cronin & Dowsett, 1991; Lambeck  
400 *et al.*, 2002). Geological evidence from deep-sea sediments and passive continental margins  
401 shows that a Pliocene sea-level highstand  $+35 \pm 18$  m above present sea levels (a.s.l.) occurred  
402 3.5–3 Ma (Cronin & Dowsett, 1991; Miller *et al.*, 2005) and swept over the emerging central  
403 Panama isthmus just prior to its final formation ~2.8 Ma (Cronin & Dowsett, 1996; Coates &  
404 Obando, 1996; O’Dea *et al.*, 2016; but see Montes *et al.*, 2015). Our divergence time estimates  
405 from MTML-msBayes place diversification in the frog assemblage around the time of this  
406 eustatic highstand (it falls within the Bayesian credible intervals completely) and match closest

407 to its lower boundary (Fig. 3).

408           To test whether a Pliocene eustatic highstand could have isolated frogs across the WPI  
409 break, we developed a GIS (geographic information systems) model of sea-level rise over a  
410 modern 250 m Digital Elevation Model using ArcMap (ESRI, Redlands, CA). Assuming the  
411 upper limit of Cronin & Dowsett (1991), the GIS sea-level model suggests a highstand  $\sim$ +50 m  
412 a.s.l. would have inundated the coastal plain between Golfo Dulce and Soná peninsula, the valley  
413 between Soná and Azuero peninsulas, and much of the east coast of Azuero peninsula, isolating  
414 it from central Panama (Fig. S3). This model is conservative, given that lower Central American  
415 lands approached their modern extent by mid-late Pliocene, and the Pliocene Panama landscape  
416 was likely lower and more topographically homogeneous (reviewed by Graham & Dilcher, 1995;  
417 Smith & Bermingham, 2005; Bagley & Johnson, 2014a). We hypothesize that the WPI break  
418 was subsequently reinforced by the mid-Pleistocene eustatic highstand  $\sim$ 550–390 ka, when sea  
419 levels were +22 m a.s.l. (Hearty *et al.*, 1999; Miller *et al.*, 2005). Relative to the dry forest  
420 hypothesis, this ‘marine vicariance hypothesis’ presents a testable and non-mutually exclusive  
421 hypothesis that explains how a eustatic highstand might have sparked multiple responses to a  
422 single period of sea-level rise and maintained any previous genetic divergence at the WPI break  
423 originally created by expansion of dry forests.

424           Within the Panamanian frog assemblage, lineage dispersal and persistence appear to be at  
425 least partly controlled by ecological requirements and degree of specialization, as well as life-  
426 history mode. For example, *E. pustulosus* is a generalist occurring in savannahs and open  
427 environments as well as humid and dry forests (Savage, 2002). In our results, this species  
428 exhibited the youngest divergence across the WPI (Fig. 3), possibly reflecting greater capacity to  
429 disperse and establish populations in different habitats, or exchange genes with other

430 populations. That said, the degree of genetic admixture among Panamanian populations of *E.*  
431 *pustulosus* is poorly understood, and has only previously been documented by nuclear allozymes  
432 (Weigt *et al.*, 2005). *Dendropsophus ebraccatus* and *A. callidryas* are ecologically similar  
433 species (Savage, 2002; Robertson *et al.*, 2009, refs. therein) and display broadly overlapping  
434  $t_{\text{MRCAS}}$  slightly older than that of *E. pustulosus* but younger than that of *C. crassidigitus* (Fig. 3).  
435 In turn, *C. crassidigitus* (like *C. talamancae*) is considered more ecologically specialized,  
436 preferring wet forest habitat more so than its dry-forest congeners (i.e. *C. fitzingeri*; Crawford *et*  
437 *al.*, 2007). That the *C. crassidigitus* gene tree extends farthest backward in time thus seems to  
438 suggest this species experienced long-term isolation and persistence in preferred habitats, rather  
439 than an ability to tolerate climatic or vegetational shifts. However, whereas all the other frog  
440 species are egg-layers, *Craugastor* dirt frogs are direct-developing species that readily  
441 reproduce, and their local population sizes can therefore be notoriously large (Crawford, 2003).  
442 Given the direct relationship between  $N_e$  and time to coalescence from coalescent theory, this  
443 contrast in life-history strategies would suggest that on one hand *C. crassidigitus* may have been  
444 superior at colonizing open niches or patches and spread throughout isthmian wet forest habitats  
445 more easily than the other taxa, while on the other hand its  $t_{\text{MRCAS}}$  estimate may also be inflated  
446 due to large ancestral  $N_e$  (Hudson, 1990).

447         Freshwater fishes typically exhibit higher levels of mtDNA sequence divergence and  
448 endemism in Atlantic relative to Pacific drainages of the Isthmus of Panama (Bermingham &  
449 Martin, 1998). On the Pacific versant, the ~124 km-wide Gulf of Panama continental shelf (Fig.  
450 1) would have been broadly exposed as eustatic sea levels lowered 110–135 m during the Last  
451 Glacial Maximum (LGM, ~21 ka) and other glaciations (e.g. Lambeck *et al.*, 2002). The above  
452 pattern likely owes to greater opportunities for dispersion and gene flow between drainages that

453 coalesced over Pacific shelf areas during Pleistocene glacial periods (Bermingham & Martin,  
454 1998; Smith & Bermingham, 2005). Yet, this trend breaks down slightly in western Panama,  
455 where freshwater fishes show distinct associations between biogeography and phylogeography.  
456 Despite low endemism within fish provinces, geographical ranges of 14 fish species terminating  
457 at Soná and Azuero peninsulas (Fig. 1) support a boundary between the Chiriquí and Santa Maria  
458 fish biogeographical provinces at the Río Santa Maria, Soná peninsula (Smith & Bermingham,  
459 2005). The WPI genetic break occurs in the same area in freshwater fishes (Fig. 2C, D). Thus,  
460 historical processes importantly shaped Panamanian fish species turnover and diversification at  
461 the WPI break zone. Yet what mechanism best explains the isolation of fishes across the WPI  
462 break?

463         The Bermingham/Martin model predicts that WPI breaks in fishes have resulted from the  
464 isolation of fish populations west of Soná peninsula from those between Soná peninsula and El  
465 Valle volcano during glacial periods with sea-level lowstands since 2 Ma in the Pleistocene  
466 (Bermingham & Martin, 1998). Consistent with this model, we found that the lower 95% HPDs  
467 for  $t_{\text{MRCA}}$  estimates for all three fish species/lineages fell within the predicted interval of  
468 diversification (Fig. 3). Peak posterior distributions from hABC model-averaging (e.g. Fig. 4)  
469 also suggested that the focal fish species/lineages most likely diversified across the WPI break  
470 1.36 Ma in the early Pleistocene, with Bayesian credible intervals ranging from early–late  
471 Pleistocene. This time period correlates best to the ‘Calabrian’ age (1.806–0.781 Ma; Gibbard *et*  
472 *al.*, 2010), a time of 41-kyr periodicity of Pleistocene glaciations, with drier and cooler-than-  
473 present conditions but less extreme climatic oscillations than those of the last 800 ka (Lambeck  
474 *et al.*, 2002; Gibbard & Kolfshoten, 2004). Nevertheless, glacial periods vastly dominated the  
475 Calabrian to present, such that the Panama isthmus would have experienced many glacio-eustatic

476 cycles but spent the majority of time since 1.8 Ma under glacial conditions with lowered sea  
477 levels and exposed continental shelf habitats. Eustatic sea-level curves give no convincing  
478 evidence that the oceans reached modern sea levels for any substantial period of time (e.g. >10–  
479 20 kyr) since the Calabrian, and the next eustatic sea-level highstand is not registered in the  
480 geological record until ~550–390 ka (Hearty *et al.*, 1999; Miller *et al.*, 2005). Geological  
481 patterns and processes are also consistent with decreased likelihood of fish dispersal across the  
482 WPI break zone since the Calabrian. In the break zone, the Pacific continental shelf becomes  
483 narrower (~0–40 km), tapering to the western Azuero peninsula coastline before being bisected  
484 by Cébaco and Coiba islands at the nearby Gulf of Montijo draining Soná peninsula (Fig. 1). To  
485 evaluate the impact of lowered sea levels during Pleistocene glaciations on drainage connectivity  
486 in this area, we obtained a GIS model predicting paths of LGM paleo-drainages over modern  
487 bathymetry using ArcMap (courtesy of Peter J. Unmack, University of Canberra). The GIS  
488 model suggests that rivers draining to the west versus east of Soná peninsula did not anastomose  
489 over the continental shelf during the LGM (Fig. 1), and possibly also preceding glaciations.  
490 Overall, our results combined with external environmental data suggest that a relatively stable  
491 geological setting at the Soná peninsula barrier has aided the historical isolation of drainage  
492 basins, maintaining fish lineage divergences at the WPI break during lower seas of the Calabrian  
493 to present.

494         While this study chiefly focuses on comparative phylogeographic modeling of  
495 codistributed Panamanian frogs and freshwater fishes, these assemblages also provide a system  
496 with ecological affinities (e.g. associations with freshwater pools and streams) and contrasts  
497 (terrestrial versus freshwater habits) making them suitable for assessing possible influences of  
498 the degree of ecological differentiation on phylogeographic structuring. One obvious ecological

499 pattern among our results is that, at the deepest phylogenetic and ecological division among taxa  
500 in our study, frogs and fishes may have experienced largely independent pulses of diversification  
501 in the WPI break zone. Divergence events in these assemblages are not entirely statistically  
502 independent, given the overlapping credible intervals of their divergence times (Figs 3 and 4),  
503 and our analyses treated these assemblages separately. However, the two-fold difference in the  
504 peak-likelihood  $E(\tau)$  estimates suggest that frogs and freshwater fishes may have responded  
505 differently to the fluctuating paleogeographic, geologic, and climatic context of western Pacific  
506 Panama (e.g. Sullivan *et al.*, 2000). We recommend that this hypothesis be tested using hABC  
507 models for comparative phylogeography improved by additional sampling and methodological  
508 improvements increasing the resolution of the models. However, under this scenario, dispersal of  
509 different lineages would be more strongly controlled by differences in ecological requirements  
510 among, rather than within, the two species assemblages. Thus, a potential biogeographical  
511 explanation for why these assemblages might have failed to register the impact of the same  
512 historical events is that the focal frog species/lineages, but not the fish lineages, colonized the  
513 Pacific coast of Costa Rica and Panama prior to the Pliocene eustatic highstand event, which left  
514 a greater signature on their genotypes than subsequent historical processes. This is supported by  
515 phylogenetic dating analyses of one frog lineage that we evaluated, the *Craugastor fitzingeri*  
516 group containing *C. crassidigitus*, which likely colonized the Central American Isthmus in the  
517 Eocene–early Miocene from a South American source population (Crawford & Smith, 2005).

## 518 **Conclusions**

519 We conducted the first tests for simultaneous diversification of frogs and fishes at the WPI break  
520 in western Panama (reviewed by Bagley & Johnson, 2014a) by analyzing mtDNA sequences  
521 using ABC methods accounting for uncertainty in model selection using modeling averaging

522 (Huang *et al.*, 2011; Hickerson *et al.*, 2014). Current findings show that, despite good prior  
523 selection and sampling properties (also supported for our datasets by simulations in Overcast *et*  
524 *al.*, 2017), hABC tests for synchronous diversification using mtDNA datasets remain challenging  
525 and difficulties can arise in conducting hypotheses tests based on Bayes factors when analyzing  
526 small numbers of taxon/population-pairs. However, our study also demonstrates that, in such  
527 cases, integrating assembly-wide divergence time estimates [ $E(\tau)$ ] from hABC with external  
528 information from geology and elevation data can still generate novel biogeographical insights  
529 and hypotheses towards refining the existing biogeographical context for a region, even despite  
530 the limitations of mtDNA (see Introduction and Appendix S1 section 3). Recent advances in  
531 hABC analysis, including extensions to genome-wide single nucleotide polymorphism (SNP)  
532 data (Xue & Hickerson, 2017) and better inference through buffering multi-taxon divergence  
533 times (Overcast *et al.*, 2017), suggest an exciting period ahead for comparative studies of the  
534 diversification of vertebrate species assemblages in Panama and other Neotropical ‘hotspots’.  
535 We encourage future phylogeographic studies of the frog and fish taxa analyzed herein, and  
536 other Panamanian taxa, to build upon the present foundation by developing and analyzing  
537 datasets with increased taxon and character sampling, while capitalizing on these computational  
538 advances. A particularly fruitful way forward in future examinations of the WPI break would be  
539 to develop SNP datasets, for example using ddRAD-seq (e.g. Peterson *et al.*, 2012), and then test  
540 for co-demographic expansion and co-diversification using aggregate site frequency spectrum  
541 methods (Xue & Hickerson, 2017). Such approaches should provide the increased power and  
542 resolution needed to more confidently identify the number and timing of divergence events that  
543 have shaped vertebrate diversification across the WPI break, and other multi-taxon genetic  
544 breaks along the Isthmus of Panama.

**545 Acknowledgements**

546 We thank María Florencia Breitman for helpful comments on earlier drafts of this manuscript.

547 We also thank the Brigham Young University Fulton Supercomputing Lab for providing

548 generous computational resources.

**549 References**

550 Arbogast, B.S. & Kenagy, G.J. 2001. Comparative phylogeography as an integrative approach to

551 historical biogeography. *J. Biogeogr.* **28**: 819-825.

552 Avise, J.C. 2000. *Phylogeography: the History and Formation of Species*. Harvard University Press,

553 Cambridge, MA.

554 Avise, J.C. 1989. Gene trees and organismal histories: a phylogenetic approach to population biology.

555 *Evolution* **43**: 1192-1208.

556 Avise, J.C., Arnold, J., Ball, R.M., Bermingham, E., Lamb, T., Neigel, J.E., Reeb, C.A. & Saunders, N.C.

557 1987. Intraspecific phylogeography: the mitochondrial DNA bridge between population genetics

558 and systematics. *Annu. Rev. Ecol. Syst.* **18**: 489-522.

559 Bagley, J.C. 2014. *Understanding the Diversification of Central American Freshwater Fishes Using*

560 *Comparative Phylogeography and Species Delimitation*. Brigham Young University, Provo, UT.

561 Bagley, J.C. 2017. PIRANHA. justincbagley/PIrANHA: PIRANHA version 0.1.4 [Data Set]. Zenodo.

562 Available at: <<http://doi.org/10.5281/zenodo.571185>>.

563 Bagley, J.C. & Hickerson, M.J. 2018. Data for: Testing hypotheses of diversification in Panamanian frogs

564 and freshwater fishes using hierarchical approximate Bayesian computation with model averaging

565 [Data Set]. Mendeley Data, v2. Available at: <<http://dx.doi.org/10.17632/f94kxmwf2n.2>>.

566 Bagley, J.C. & Johnson, J.B. 2014a. Phylogeography and biogeography of the lower Central American

567 Neotropics: diversification between two continents and between two seas. *Biol. Rev.* **89**: 767-790.

568 Bagley, J.C. & Johnson, J.B. 2014b. Testing for shared biogeographic history in the lower Central

569 American freshwater fish assemblage using comparative phylogeography: concerted,

570 independent, or multiple evolutionary responses? *Ecol. Evol.* **4**: 1686-1705.

571 Beaumont, M.A., Zhang, W. & Balding, D.J. 2002. Approximate Bayesian computation in population

572 genetics. *Genetics* **162**: 2025-2035.

573 Bermingham, E. & Avise, J.C. 1986. Molecular zoogeography of freshwater fishes in the south-eastern

574 United States. *Genetics*, **113**: 939-965.

- 575 Bermingham, E. & Martin, A.P. 1998. Comparative mtDNA phylogeography of Neotropical freshwater  
576 fishes: testing shared history to infer the evolutionary landscape of lower Central America. *Mol.*  
577 *Ecol.* **7**: 499-517.
- 578 BurrIDGE, C.P., Craw, D., Fletcher, D. & Waters, J.M. 2008. Geological dates and molecular rates: fish  
579 DNA sheds light on time dependency. *Mol. Biol. Evol.* **18**: 624-633.
- 580 Burnham, R.J. & Graham, A. 1999. The history of neotropical vegetation: new developments and status.  
581 *Ann. Missouri Bot. Gard.* **86**: 546-589.
- 582 Bussing, W.A. 1976. Geographic distribution of the San Juan ichthyofauna of Central America with  
583 remarks on its origin and ecology. In: *Investigations of the Ichthyofauna of Nicaraguan Lakes*  
584 (T.B. Thorson, ed.), pp. 157-175. University of Nebraska, Lincoln, NE.
- 585 Bussing, W.A. 1998. *Freshwater Fishes of Costa Rica*, 2nd Edn. Editorial de la Universidad de Costa  
586 Rica, San José, Costa Rica.
- 587 Coates, A.G. & Obando, J.A. 1996. The geologic evolution of the Central American isthmus. In:  
588 *Evolution and Environment in Tropical America* (J.B.C. Jackson, A.F. Budd & A.G. Coates, eds),  
589 pp. 21-56. University of Chicago Press, Chicago, IL.
- 590 Crawford, A.J., Bermingham, E. & Polania, C. 2007. The role of tropical dry forest as a long-term barrier  
591 to dispersal: a comparative phylogeographical analysis of dry forest tolerant and intolerant frogs.  
592 *Mol. Ecol.* **16**: 4789-4807.
- 593 Crawford, A.J. & Smith, E.N. 2005. Cenozoic biogeography and evolution in direct developing frogs of  
594 Central America (Leptodactylidae: *Eleutherodactylus*) as inferred from a phylogenetic analysis of  
595 nuclear and mitochondrial genes. *Mol. Phylogenet. Evol.* **35**: 536-555.
- 596 Cronin, T.M. & Dowsett, H.J. (guest editors). 1991. Pliocene Climates. *Quatern. Sci. Rev.* **10**: 115-296.
- 597 Dolman, G. & Joseph, L. 2012. A species assemblage approach to comparative phylogeography of birds  
598 in southern Australia. *Ecol. Evol.* **2**: 354-369.
- 599 Drummond, A.J., Ho, S.Y.W., Phillips, M.J. & Rambaut, A. 2006. Relaxed phylogenetics and dating with  
600 confidence. *PLoS Biol.* **4**: e88.
- 601 Drummond, A.J., Suchard, M.A., Xie, D. & Rambaut, A. 2012. Bayesian phylogenetics with BEAUti and  
602 the BEAST 1.7. *Mol. Biol. Evol.* **29**: 1969-1973.
- 603 Edwards, S.V. & Beerli, P. 2000. Perspective: gene divergence, population divergence, and the variance  
604 in coalescence time in phylogeographic studies. *Evolution* **54**: 1839-1854.
- 605 Gibbard, P.L., Head, M.J., Walker, M.J.C. & The Subcommittee on Quaternary Stratigraphy. 2010.  
606 Formal ratification of the Quaternary System/Period and the Pleistocene Series/Epoch with a base  
607 at 2.58 Ma. *J. Quaternary Sci.* **25**: 96-102.

- 608 Gibbard, P. & van Kolfschoten, T. 2004. The Pleistocene and Holocene epochs. In: *A Geologic Time*  
609 *Scale 2004* (F.M. Gradstein, J.G. Ogg & A.G. Smith, eds), pp. 441-452. Cambridge University  
610 Press, Cambridge, UK.
- 611 Graham, A. & Dilcher, D. 1995. The Cenozoic record of tropical dry forest in northern Latin America and  
612 the southern United States. In: *Seasonally Dry Tropical Forests* (S.H. Bullock, H.A. Mooney &  
613 E. Medina, eds), pp. 124-145. Cambridge University Press, Cambridge, UK.
- 614 Hasegawa, M., Kishino, H. & Yano, T. 1985. Dating of the human-ape splitting by a molecular clock of  
615 mitochondrial DNA. *J. Mol. Evol.* **22**: 160-174.
- 616 Hearty, P.J., Kindler, P., Cheng, H. & Edwards, R.L. 1999. A +20 m middle Pleistocene sea-level  
617 highstand (Bermuda and the Bahamas) due to partial collapse of Antarctic ice. *Geology* **27**: 375-  
618 378.
- 619 Heled, J. & Drummond, A.J. 2010. Bayesian inference of species trees from multilocus data. *Mol. Biol.*  
620 *Evol.* **27**: 570-580.
- 621 Hey, J. & Machado, C.A. 2003. The study of structured populations—new hope for a difficult and  
622 divided science. *Nat. Rev. Genet.* **4**: 535-543.
- 623 Hickerson, M.J., Carstens, B.C., Cavender-Bares, J., Crandall, K.A., Graham, C.H., Johnson, J.B.,  
624 Rissler, L., Victoriano, P.F. & Yoder, A.D. 2010. Phylogeography's past, present, and future: 10  
625 years after Avise, 2000. *Mol. Phylogenet. Evol.* **54**: 291-301.
- 626 Hickerson, M.J., Stahl, E. & Lessios, H.A. 2006. Test for simultaneous divergence using Approximate  
627 Bayesian Computation. *Evolution* **60**: 2435-2453.
- 628 Hickerson, M.J., Stahl, E. & Takebayashi, N. 2007. msBayes: a pipeline for testing comparative  
629 phylogeographic histories using hierarchical approximate Bayesian computation. *BMC*  
630 *Bioinformatics* **8**: 268.
- 631 Hickerson, M.J., Stone, G.N., Lohse, K., Demos, T.C., Xie, X., Landerer, C. & Takebayashi, N. 2014.  
632 Recommendations for using msBayes to incorporate uncertainty in selecting an ABC model prior:  
633 a response to Oaks *et al.* *Evolution* **68**: 284-294.
- 634 Huang, W., Takebayashi, N., Qi, Y. & Hickerson, M.J. 2011. MTML-msBayes: Approximate Bayesian  
635 comparative phylogeographic inference from multiple taxa and multiple loci with rate  
636 heterogeneity. *BMC Bioinformatics* **12**: 1.
- 637 Hudson, R.R. 1990. Gene genealogies and the coalescent process. *Oxford Surv. Evol. Biol.* **7**: 1-44.
- 638 Irwin, D.E. 2012. Local adaptation along smooth ecological gradients causes phylogeographic breaks and  
639 phenotypic clustering. *Am. Nat.* **180**: 35-49.
- 640 Jeffreys, H. 1961. *Theory of Probability*, 3rd edn. Clarendon, Oxford, UK.
- 641 Kass, R.E. & Raftery, A.E. 1995. Bayes Factors. *J. Am. Stat. Assoc.* **90**: 773-795.

- 642 Kidd, D.M. & Ritchie, M.G. 2006. Phylogeographic information systems: putting the geography into  
643 phylogeography. *J. Biogeogr.* **33**: 1851-1865.
- 644 Kingman, J. 1982. The coalescent. *Stoch. Proc. Appl.* **13**: 235-248.
- 645 Kubatko, L.S., Carstens, B.C. & Knowles, L.L. 2009. STEM: species tree estimation using maximum  
646 likelihood for gene trees under coalescence. *Bioinformatics* **25**: 971-973.
- 647 Kuo, C.H. & Avise, J.C. 2005. Phylogeographic breaks in low-dispersal species: the emergence of  
648 concordance across gene trees. *Genetica* **124**: 179-186.
- 649 Lambeck, K., Esat, T.M. & Potter, E.K. 2002. Links between climate and sea levels for the past three  
650 million years. *Nature* **419**: 199-206.
- 651 Leaché, A.D., Crews, S.C. & Hickerson, M.J. 2007. Two waves of diversification in mammals and  
652 reptiles of Baja California revealed by hierarchical Bayesian analysis. *Biol. Letters* **3**: 646-650.
- 653 Librado, P. & Rozas, J. 2009. DnaSP v5: a software for comprehensive analysis of DNA polymorphism  
654 data. *Bioinformatics* **25**: 1451-1452.
- 655 Macey, J.R., Schulte II, J.A., Larson, A., Fang, Z., Wang, Y., Tuniyev, B.S. & Papenfuss, T.J. 1998.  
656 Phylogenetic relationships of toads in the *Bufo bufo* species group from the Eastern Escarpment  
657 of the Tibetan Plateau: a case of vicariance and dispersal. *Mol. Phylogenet. Evol.* **9**: 80-87.
- 658 Martin, A.P. & Bermingham, E. 2000. Regional endemism and cryptic species revealed by molecular and  
659 morphological analysis of a widespread species of Neotropical catfish. *Proc. R. Soc. Lond. B* **267**:  
660 1135-1141.
- 661 McCafferty, S.S., Martin, A. & Bermingham, E. 2012. Phylogeographic diversity of the lower Central  
662 American cichlid *Andinoacara coeruleopunctatus* (Cichlidae). *Int. J. Evol. Biol.* **2012**: Article ID  
663 780169.
- 664 McDonald, J.H. & Kreitman, M. 1991. Adaptive protein evolution at the *Adh* locus in *Drosophila*. *Nature*  
665 **351**: 652-654.
- 666 Miller, K.G., Kominz, M.A., Browning, J.V., Wright, J.D., Mountain, G.S., Katz, M.E., Sugarman, P.J.,  
667 Cramer, B.S., Christie-Blick, N. & Pekar, S.F. 2005. The Phanerozoic record of global sea-level  
668 change. *Science* **310**: 1293-1298.
- 669 Montes, C., Cardona, A., Jaramillo, C., Pardo, A., Silva, J.C., Valencia, V., Ayala, C., Pérez-Angel, L.C.,  
670 Rodríguez-Parra, L.A., Ramirez, V. & Niño, H. 2015. Middle Miocene closure of the Central  
671 American seaway. *Science* **348**: 226-229.
- 672 Nei, M. 1987. *Molecular Evolutionary Genetics*. Columbia University Press, New York.
- 673 Oaks, J.R. 2014. An improved approximate-Bayesian model-choice method for estimating shared  
674 evolutionary history. *BMC Evol. Biol.* **14**: 150.

- 675 Oaks, J.R., Linkem, C.W. & Sukumaran, J. 2014. Implications of uniformly distributed, empirically  
676 informed priors for phylogeographical model selection: A reply to Hickerson *et al.* *Evolution* **68**:  
677 3607-3617.
- 678 Oaks, J.R., Sukumaran, J., Esselstyn, J.A., Linkem, C.W., Siler, C.D., Holder, M.T. & Brown, R.M. 2013.  
679 Evidence for climate-driven diversification? A caution for interpreting ABC inferences of  
680 simultaneous historical events. *Evolution* **67**: 991-1010.
- 681 O’Dea, A., Lessios, H.A., Coates, A.G., Eytan, R.I., Restrepo-Moreno, S.A., Cione, A.L., Collins, L.S.,  
682 de Queiroz, A., Farris, D.W., Norris, R.D. & Stallard, R.F. 2016. Formation of the Isthmus of  
683 Panama. *Sci. Adv.* **2**: e1600883.
- 684 Overcast, I., Bagley, J.C. & Hickerson, M.J. 2017. Improving approximate Bayesian computation tests for  
685 synchronous diversification by buffering divergence time classes. *BMC Evolutionary Biology* **17**:  
686 203.
- 687 Papadopoulou, A. & Knowles, L.L. 2015. Species-specific responses to island connectivity cycles:  
688 refined models for testing phylogeographic concordance across a Mediterranean Pleistocene  
689 Aggregate Island Complex. *Mol. Ecol.* **24**: 4252-4268.
- 690 Perdices, A., Bermingham, E., Montilla, A. & Doadrio, I. 2002. Evolutionary history of the genus  
691 *Rhamdia* (Teleostei: Pimelodidae) in Central America. *Mol. Phylogenet. Evol.* **25**: 172-189.
- 692 Perdices, A., Doadrio, I. & Bermingham, E. 2005. Evolutionary history of the synbranchid eels  
693 (Teleostei: Synbranchidae) in Central America and the Caribbean islands inferred from their  
694 molecular phylogeny. *Mol. Phylogenet. Evol.* **37**: 460-473.
- 695 Peterson, B.K., Weber, J.N., Kay, E.H., Fisher, H.S. & Hoekstra, H.E. 2012. Double digest RADseq: an  
696 inexpensive method for de novo SNP discovery and genotyping in model and non-model species.  
697 *PLoS One* **7**: e37135.
- 698 Picq, S., Alda, F., Krahe, R. & Bermingham, E. 2014. Miocene and Pliocene colonization of the Central  
699 American Isthmus by the weakly electric fish *Brachyhypopomus occidentalis* (Hypopomidae,  
700 Gymnotiformes). *J. Biogeogr.* **41**: 1520-1532.
- 701 Piperno, D.R. & Pearsall, D.M. 1998. *The Origins of Agriculture in the Lowland Neotropics*. Academic  
702 Press, San Diego, CA.
- 703 Reeves, R.G. & Bermingham, E. 2006. Colonization, population expansion, and lineage turnover:  
704 phylogeography of Mesoamerican characiform fish. *Biol. J. Linn. Soc.* **88**: 235-255.
- 705 Riddle, B.R., Dawson, M.N., Hadly, E.A., Hafner, D.J., Hickerson, M.J., Mantooth, S.J. & Yoder, A.D.  
706 2008. The role of molecular genetics in sculpting the future of integrative biogeography. *Prog.*  
707 *Phys. Geog.* **32**: 173-202.

- 708 Riddle, B.R. & Hafner, D.J. 2006. A step-wise approach to integrating phylogeographic and phylogenetic  
709 biogeographic perspectives on the history of a core North American warm desert biota. *J. Arid*  
710 *Environ.* **66**: 435-461.
- 711 Robertson, J.M., Duryea, M.C. & Zamudio, K.R. 2009. Discordant patterns of evolutionary  
712 differentiation in two Neotropical treefrogs. *Mol. Ecol.* **18**: 1375-1395.
- 713 Robertson, J.M. & Zamudio, K.R. 2009. Genetic diversification, vicariance, and selection in a polytypic  
714 frog. *J. Heredity* **100**: 715-731.
- 715 Savage, J.M. 1966. The origins and history of the Central American herpetofauna. *Copeia* **1966**: 719-766.
- 716 Savage, J.M. 1982. The enigma of the Central American herpetofauna: dispersals or vicariance? *Ann. Mo.*  
717 *Bot. Gard.* **69**: 464-547.
- 718 Savage, J.M. 2002. *The Amphibians and Reptiles of Costa Rica: a Herpetofauna Between Two*  
719 *Continents, Between Two Seas*. University of Chicago Press, Chicago, IL.
- 720 Smith, S.A. & Bermingham, E. 2005. The biogeography of lower Mesoamerican freshwater fishes. *J.*  
721 *Biogeogr.* **32**: 1835-1854.
- 722 Soltis, D.E., Morris, A.B., Jason, M., McLachlan, S., Manos, P.S. & Soltis, P.S. 2006. Comparative  
723 phylogeography of unglaciated eastern North America. *Mol. Ecol.* **15**: 4261-4293.
- 724 Sullivan, J., Arellano, E. & Rogers, D. 2000. Comparative phylogeography of Mesoamerican highland  
725 rodents: concerted versus independent response to past climatic fluctuations. *Am. Nat.* **155**: 755-  
726 768.
- 727 Swofford, D.S. 2002. *PAUP\*: Phylogenetic analysis using parsimony (\*and other methods), version*  
728 *4.0b10*. Sinauer, Sunderland, MA.
- 729 Vanzolini, P.E. & Heyer, W.R. 1985. The American herpetofauna and the interchange. In: *The Great*  
730 *American Biotic Interchange* (F.G. Stehli & S.D. Webb, eds), pp. 475-487. Plenum Press, New  
731 York.
- 732 Wang, I.J., Crawford, A.J. & Bermingham, E. 2008. Phylogeography of the pygmy rain frog (*Pristimantis*  
733 *ridens*) across the lowland wet forests of isthmian Central America. *Mol. Phylogenet. Evol.* **47**:  
734 992-1004.
- 735 Waters, J.M. & Burrige, C.P. 1999. Extreme intraspecific mitochondrial DNA sequence divergence in  
736 *Galaxias maculatus* (Osteichthys: Galaxiidae), one of the world's most widespread freshwater  
737 fish. *Mol. Phylogenet. Evol.* **11**: 1-12.
- 738 Weigt, L.A., Crawford, A.J., Rand, A.S. & Ryan, M.J. 2005. Biogeography of the túngara frog,  
739 *Physalaemus pustulosus*: a molecular perspective. *Mol. Ecol.* **14**: 3857-3876.
- 740 Xue A.T. & Hickerson, M.J. 2015. The aggregate site frequency spectrum for comparative population  
741 genomic inference. *Mol. Ecol.* **24**: 6223-6240.

- 742 Xue, A.T. & Hickerson, M.J. 2017. Multi-DICE: R package for comparative population genomic  
743 inference under hierarchical co-demographic models of independent single-population size  
744 changes. *Mol. Ecol. Resour.* **17**: e212-e224.
- 745 Zeh, J.A., Zeh, D.W. & Bonilla, M.M. 2003. Phylogeography of the harlequin beetle-riding  
746 pseudoscorpion and the rise of the Isthmus of Panama. *Mol. Ecol.* **12**: 2759-2769.
- 747 Zink, R.M. 2002. Methods in comparative phylogeography, and their application to studying evolution in  
748 the North American Aridlands. *Integr. Comp. Biol.* **42**: 953-959.
- 749 Zink, R.M. & Barrowclough, G.F. 2008. Mitochondrial DNA under siege in avian phylogeography. *Mol.*  
750 *Ecol.* **17**: 2107-2121.

**Table 1** (on next page)

List of taxa used to examine temporal diversification patterns across the western Panama isthmus.

For multi-gene datasets, total alignment length is given in nucleotide base pairs (bp) followed by length of each gene in parentheses, in the same order genes are listed at left. The transition/transversion ratios (Ti/Tv; i.e. kappa parameters) are HKY+ $\Gamma$ +I model estimates, and percent genetic divergences (% div) are given as average pairwise HKY+ $\Gamma$ +I distances between population-pairs.  $\pi$ , nucleotide diversity (Nei, 1987).

	mtDNA genes	Length (bp)	$n_{\text{total}}$ (west/east)	$\pi$	Ti/Tv	% div	Source
Frogs							
<i>Agalychnis callidryas</i>	<i>16S, NDI</i>	1149 (118, 1031)	28 (16/12)	0.0337	11.373	8.0	Robertson & Zamudio (2009)
<i>Craugastor crassidigitus</i>	<i>cytb, cox1</i>	1353 (714, 639)	13 (5/8)	0.0645	14.55	13.9	Crawford <i>et al.</i> (2007)
<i>Dendropsophus ebraccatus</i>	<i>NDI, tRNAs</i>	1877	18 (11/7)	0.0245	12.04	5.9	Robertson <i>et al.</i> (2009)
<i>Physalaemus pustulosus</i>	<i>cox1</i>	564	15 (2/13)	0.0139	31.67	4.6	Weigt <i>et al.</i> (2005)
Freshwater fishes							
<i>Andinoacara coeruleopunctatus</i>	<i>ATP6/8</i>	842	10 (2/8)	0.0093	20.77	2.4	McCafferty <i>et al.</i> (2012)
<i>Pimelodella chagresi</i>	<i>ATP6/8, cox1</i>	1471 (842, 629)	14 (6/8)	0.0210	12.19	3.5	Bermingham & Martin (1998)
<i>Roeboides occidentalis-R. guatemalensis</i>	<i>ATP6/8, cox1</i>	1493 (842, 651)	11 (8/3)	0.0311	10.36	6.4	Bermingham & Martin (1998)

**Table 2** (on next page)

Prior model classes and results of tests for synchronous diversification using ABC model averaging in MTML-msBayes.

Parameters are shown for four prior model classes ran for each of two analyses of  $Y$  population-pairs used to test for synchronous diversification across the WPI break. Prior models had varying  $\tau$ ,  $\theta_D$ , and  $\theta_A$  prior distributions,  $P(x)$ , but assumed zero post-divergence migration. Approximate posterior probabilities  $P(M_k|D)^{1000}$  of each model are given based on 1000 accepted simulated draws from 20 million random draws from the four prior models, with that of the best-supported model underlined. Modal  $\Omega$  hyper-parameter estimates and their 95% highest posterior densities (HPDs) from model averaging over all four prior models are given in the first row of each section.

Prior	$P(\tau)$	$P(\theta_D)$	$P(\theta_A)$	$P(M_k D)^{1000}$	$\Omega$ mode	$\Omega$ 95% HPDs
WPI frogs ( $Y = 4$ )					0.0036	[0.000, 0.0565]
$M_1$	$\sim U(0, 1.75)$	$\sim U(0, 0.1)$	$\sim U(0, 0.25)$	0.2666	–	–
$M_2$	$\sim U(0, 1.75)$	$\sim U(0, 0.1)$	$\sim U(0, 0.5)$	<u>0.4990</u>	–	–
$M_3$	$\sim U(0, 1.75)$	$\sim U(0, 0.4)$	$\sim U(0, 0.25)$	0.0000	–	–
$M_4$	$\sim U(0, 0.875)$	$\sim U(0, 0.1)$	$\sim U(0, 0.25)$	0.2344	–	–
WPI fishes ( $Y = 3$ )					0.0017	[0.000, 0.0423]
$M_1$	$\sim U(0, 0.8)$	$\sim U(0, 0.1)$	$\sim U(0, 0.25)$	0.3124	–	–
$M_2$	$\sim U(0, 0.8)$	$\sim U(0, 0.1)$	$\sim U(0, 0.5)$	<u>0.3766</u>	–	–
$M_3$	$\sim U(0, 0.8)$	$\sim U(0, 0.4)$	$\sim U(0, 0.25)$	0.0000	–	–
$M_4$	$\sim U(0, 0.4)$	$\sim U(0, 0.1)$	$\sim U(0, 0.25)$	0.3110	–	–

**Figure 1**(on next page)

Map of the study area.

The western Panama isthmus (WPI) break zone is shaded gray, and major physiographic features including the continental divide, peninsulas, and mountain ranges are shown over a digital elevation layer; GC, Golfo de Chiriquí; GM, Golfo de Montijo. Paleo-bathymetric river paths modeled assuming a 135 m eustatic sea level drop during the Last Glacial Maximum using ArcMap (ESRI, Redlands, CA; courtesy of Peter J. Unmack) are shown with the  $-135$  m bathymetric contour (dashed line) as a reference.

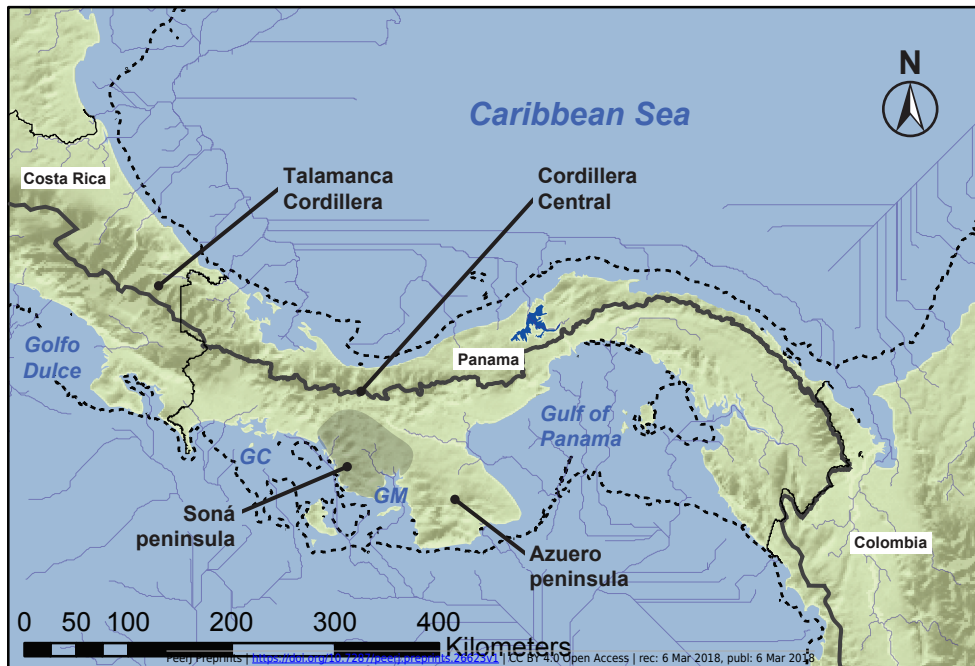
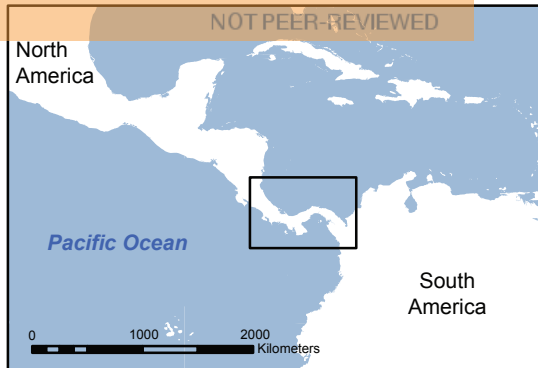
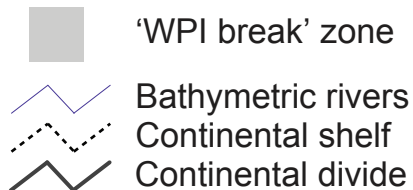


**Figure 2** (on next page)

Geographical locations of WPI phylogeographic breaks registered in different species/lineages of Panamanian (A, B) frogs and (C, D) freshwater fishes evaluated in this study.

Map features and lines are identical to those in Fig. 1.

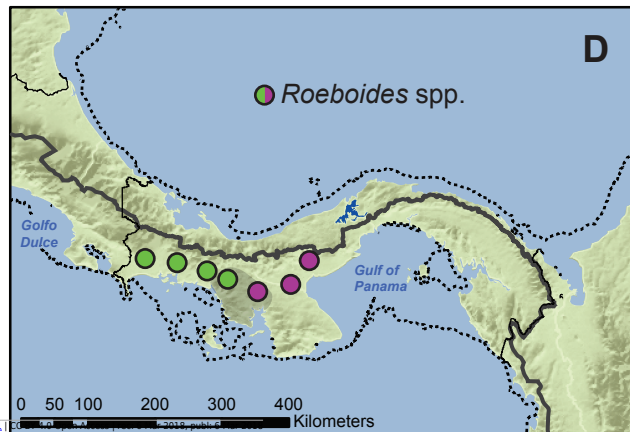
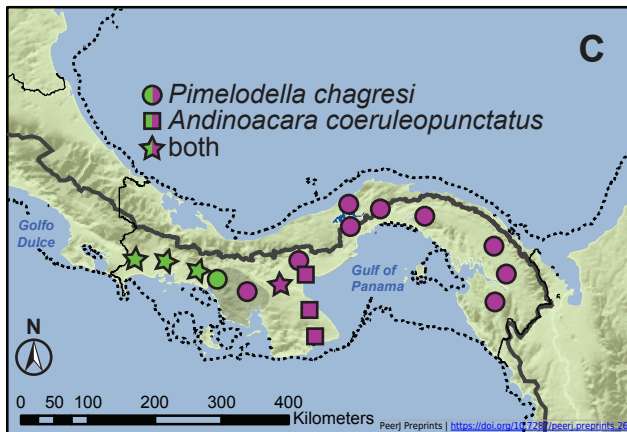
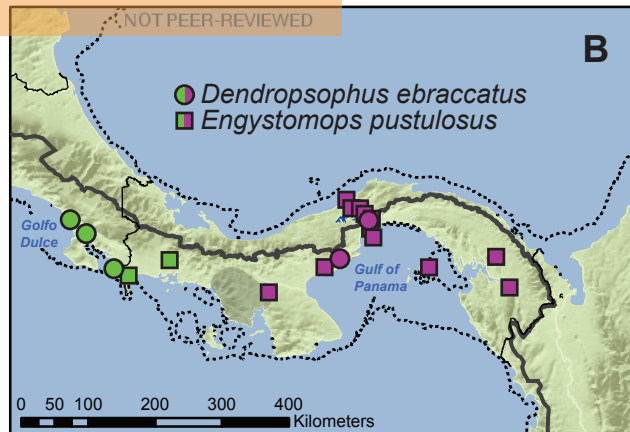
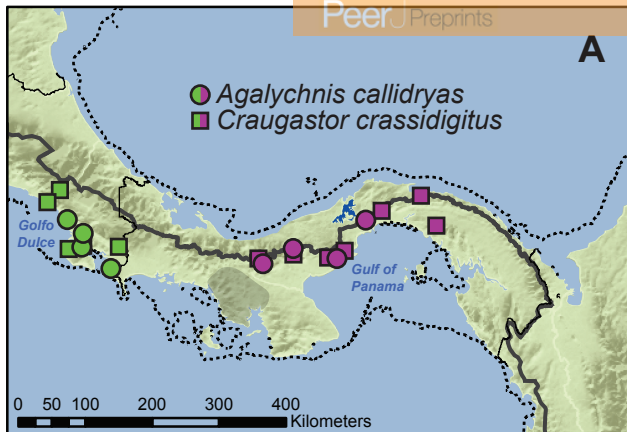
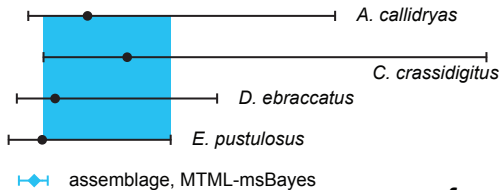


**Figure 3**(on next page)

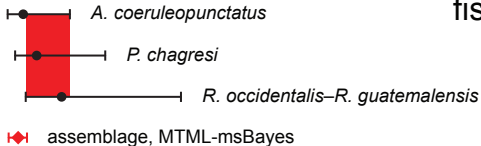
Comparison of divergence time estimates for species/lineages, and species assemblages, diverged across the WPI break.

Species/lineage gene-tree depths ( $t_{\text{MRCA}s}$ ) from BEAST (Drummond *et al.*, 2012; corresponding to tree depths in Fig. S1) are shown as geometric means (dots) and 95% HPDs, with regions of overlap in coalescence times shaded gray. Estimated times of assemblage co-divergences are shown as modal/peak posterior estimates (diamonds) and 95% HPDs from ABC model averaging in MTML-msBayes.

Taxa



frogs



fishes

0 10 20 30 40

Time (millions of years ago, Ma)

**Figure 4**(on next page)

Hierarchical approximate Bayesian computation (hABC) results.

Joint hyper-posterior probability distributions of the mean divergence time,  $E(\tau)$  (left x-axis, coalescent time; right x-axis, absolute time), and the dispersion index of divergence times,  $\Omega$ , from MTML-msbayes (Huang *et al.*, 2011) are presented for (A) frogs and (B) freshwater fishes based on ABC model-averaging across model classes. Inset graphs show the posterior densities of  $\Omega$  from each analysis.

